A Morphogenesis Checkpoint Monitors the Actin Cytoskeleton in Yeast

John N. McMillan, Rey A.L. Sia, and Daniel J. Lew

Department of Pharmacology and Cancer Biology, Duke University Medical Center, Durham, North Carolina 27710

Abstract. A morphogenesis checkpoint in budding yeast delays cell cycle progression in response to perturbations of cell polarity that prevent bud formation (Lew, D.J., and S.I. Reed. 1995. *J. Cell Biol.* 129:739–749). The cell cycle delay depends upon the tyrosine kinase Swe1p, which phosphorylates and inhibits the cyclin-dependent kinase Cdc28p (Sia, R.A.L., H.A. Herald, and D.J. Lew. 1996. *Mol. Biol. Cell.* 7:1657–1666). In this report, we have investigated the nature of the defect(s) that trigger this checkpoint. A Swe1p-dependent cell cycle delay was triggered by direct perturbations of the actin cytoskeleton, even when polarity establishment functions remained intact. Furthermore, actin perturbation could trigger the checkpoint even in cells that had already formed a bud, suggesting that the checkpoint directly monitors actin organization, rather than (or in addition to) polarity establishment or bud formation. In addition, we show that the checkpoint could detect actin perturbations through most of the cell cycle. However, the ability to respond to such perturbations by delaying cell cycle progression was restricted to a narrow window of the cell cycle, delimited by the periodic accumulation of the checkpoint effector, Swe1p.

Key words: checkpoint • actin • SWE1 • morphogenesis • cell cycle

PROLIFERATING cells must coordinate cell cycle events so that they occur in the proper order with respect to each other. Insight into how disparate processes such as DNA replication, spindle formation, and cytokinesis are coordinated came from the discovery of surveillance pathways called checkpoint controls (Hartwell and Weinert, 1989; Murray, 1992). Checkpoint controls are regulatory pathways that monitor the progress of key cell cycle events and act to delay cell cycle progression if those events have not been satisfactorily completed. For instance, the DNA replication checkpoint delays entry into mitosis until DNA replication is complete, whereas the spindle assembly checkpoint delays anaphase onset until all of the chromosomes are properly oriented on the mitotic spindle. Thus, checkpoint controls ensure that cell cycle events occur in the proper order even if some perturbation delays performance of a particular event.

How do checkpoint controls sense the progress of cell cycle events? The DNA replication checkpoint is thought to monitor the status of DNA replication forks; these are disassembled when DNA replication is complete, so their presence indicates incomplete (or stalled) DNA replication, prompting the checkpoint to delay cell cycle progression (Li and Deshaies, 1993; Navas et al., 1995). The spindle assembly checkpoint appears to monitor the status of kinetochores on mitotic chromosomes: the composition of kinetochores changes upon attachment to the spindle (Nicklas et al., 1995; Wells, 1996), so the presence of unattached (or improperly attached) kinetochores indicates incomplete spindle assembly, prompting the checkpoint to delay cell cycle progression.

A slightly different checkpoint paradigm is provided by the DNA damage checkpoint. Rather than monitoring a particular cell cycle event, this checkpoint monitors DNA damage, which can occur as a result of extrinsic factors at any time in the cell cycle. Depending on the time within the cell cycle at which the DNA damage is incurred, the checkpoint can exert different effects on cell cycle progression, promoting a delay in G1, a slowing of S phase, a G2 arrest, or even a pause in midanaphase (Weinert and Hartwell, 1988; Siede et al., 1993; Paulovich and Hartwell, 1995; Yang et al., 1997; for review see Lew et al., 1997). These delays are thought to preserve genome integrity by allowing time for repair of the damage before cell cycle events like DNA replication or chromosome segregation render the damage unrepairable.

In yeast, a morphogenesis checkpoint delays nuclear division when cell polarity is perturbed (Lew and Reed, 1995*a*). Environmental stresses, such as increases in tem-

Address all correspondence to Daniel J. Lew, Room C359 LSRC, Box 3686, Department of Pharmacology and Cancer Biology, Duke University Medical Center, Durham, NC 27710. Tel.: (919) 613-8627. Fax: (919) 613-8642. E-mail: daniel.lew@duke.edu

perature or osmolarity, cause a temporary disruption of cytoskeletal polarity and delay bud formation (Chowdhury et al., 1992; Lillie and Brown, 1994). During this delay, cell cycle progression is halted, preventing the accumulation of binucleate cells. The cell cycle arrest is due to inhibitory phosphorylation of the master cell cycle regulatory cyclin-dependent kinase, Cdc28p, at tyrosine 19 (Lew and Reed, 1995*a*). This lowers the activity of G2 cyclin–Cdc28p complexes, preventing nuclear division. Phosphorylation of Cdc28p is catalyzed by the protein kinase Swe1p (Booher et al., 1993); cells lacking Swe1p are unable to delay mitosis in response to depolarizing conditions and thus become binucleate (Sia et al., 1996). The structure(s) monitored by the morphogenesis checkpoint has not yet been described and forms the subject of this report.

Unbudded yeast cells in G1 are triggered to initiate bud formation by the activation of G1 cyclin–Cdc28p complexes (Cdc28p is homologous to cdc2 in fission yeast) (Lew and Reed, 1993). Bud formation also requires the activation (GTP loading) of the Rho-family GTPase, Cdc42p, catalyzed by the guanine nucleotide exchange factor Cdc24p (Fig. 1) (Pringle et al., 1995). In a manner that is poorly understood, activation of Cdc28p and Cdc42p leads to polarization of the actin cytoskeleton, assembly of septin filaments, and polarization of various cortical proteins towards a "prebud site" from which the bud will emerge (Fig. 1). This site is dictated by positional information encoded and interpreted by a set of "bud site selection" genes (Fig. 1) (Pringle et al., 1995). Polarized actin cables are thought to provide tracks along which secretory vesicles are delivered to the prebud site (Novick and Botstein, 1985), and septin filaments are thought to provide scaffolds for the local activation of specific cell wall synthesis enzymes (DeMarini et al., 1997). Together, the polarization of secretory and cell wall synthetic activities result in bud formation (Fig. 1).

In previous studies, the morphogenesis checkpoint was investigated primarily through the use of temperature-sensitive *cdc24* and *cdc42* mutants (Lew and Reed, 1995*a*; Sia et al., 1996). At the restrictive temperature, these mutants prevent activation of Cdc42p, and hence polarization of all cytoskeletal elements, leading to a failure in bud formation (Adams et al., 1990). Since so many events were blocked in these mutants, it was impossible to distinguish whether the checkpoint monitored an upstream event in polarity establishment (such as GTP loading of Cdc42p), an intermediate step (such as actin polarization), or the final outcome (the presence or size of a bud). In this report, we have used a panel of other mutants as well as the actin depolymerizing drug latrunculin-A (Lat-A)[1] to investigate the defect monitored by the morphogenesis checkpoint. The results suggest that the checkpoint monitors actin organization. Furthermore, while perturbation of actin can be detected by the checkpoint throughout the period of bud formation, it is only translated into a cell cycle delay if the perturbation occurs during the critical early phase of bud formation. This restriction is due to the periodic expression of the checkpoint effector, Swe1p.

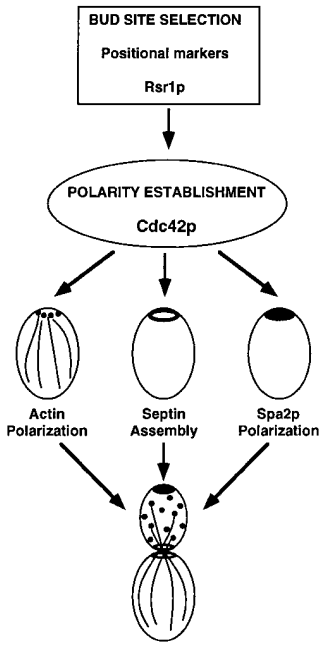

Figure 1. Establishment of cell polarity in yeast. Bud site selection genes establish a future bud site at a location that depends on the mating type of the cell. Cdc42p becomes concentrated at that site and promotes the polarization of the actin cytoskeleton towards that site, as well as the assembly of septin filaments and the concentration of cortical proteins (e.g., Spa2p) at that site. 10–20 min after polarization, the cells make a visible bud, which then grows through directed secretion dependent upon polarized actin (for reviews see Lew and Reed, 1995*b*; Pringle et al., 1995; Lew et al., 1997).

Materials and Methods

Reagents

Rhodamine-conjugated phalloidin was purchased from Molecular Probes (Eugene, OR) and stored as a 200 U/ml stock solution in methanol at −20°C. 4′6′-diamidino-2-phenylindole (DAPI) was purchased from Sigma Chemical Co. (St. Louis, MO) and stored as a 1 mg/ml stock solution in H_2O at −20°C. Lat-A was initially provided as a generous gift by David Drubin (University of California, Berkeley, CA) and subsequently purchased from Molecular Probes and stored as a 20 mM stock solution in dimethylsulfoxide at −20°C. 9E10 monoclonal anti-myc antibody was purchased from Santa Cruz Biotechnology, Inc. (Santa Cruz, CA). Monoclonal anti-PSTAIRE antibody was a gift from Dr. Steven Reed (The Scripps Research Institute, La Jolla, CA). HRP-conjugated goat anti–mouse secondary antibody was purchased from Jackson ImmunoResearch Laboratories, Inc. (West Grove, PA). Mounting medium was made as described (Pringle et al., 1991).

Yeast Strains, Growth Conditions, and Cell Synchrony

The yeast strains used in this study are listed in Table I. All are in the BF264-15DU background (*ade1*, *his2*, *leu2-3,112*, *trp1-1*^{a}, *ura3Δns*). Gene disruptions (*cap2::URA3* [Cannon and Tatchell, 1987; Amatruda et al., 1990], *tpm1::URA3* [Liu and Bretscher, 1989], *sac6::URA3* [Adams et al., 1991], *swe1::LEU2* [Booher et al., 1993], and *mih1::LEU2* [Russell et al., 1989]) and the *GAP::SWE1* allele (Sia et al., 1996) were constructed by direct transformation into the BF264-15DU background. Other alleles (*myo2-66* [Johnston et al., 1991], *pfy1-111::LEU2* [Haarer et al., 1993], and *cdc15-2* [Hartwell et al., 1974]) were serially backcrossed a minimum of six times into the BF264-15DU background.

The *SWE1-myc* construct was generated as follows: a 3.7-kb XbaI-BamHI fragment from pSWE1-HA (Booher et al., 1993) containing *GAL1-SWE1-HA* was cloned into an altered version of pRS306 (Sikorski and Hieter, 1989), which had the polylinker sites from KpnI to SmaI deleted. The NheI site in the HA tag sequence was converted into a SalI site using the linker oligonucleotide 5′-CTAGCGTCGACA-3′, and a 400-bp XhoI-SalI fragment containing 12 tandem copies of the myc epitope (Paul Russell, The Scripps Research Institute) was cloned into the SalI site. To create the *SWE1-myc* strain RSY206, the construct was digested with KpnI, which cuts near the COOH terminus of *SWE1*, directing integration at the *SWE1* locus in yeast. This results in a tagged *SWE1* on its own promoter, with an adjacent *URA3* marker and *GAL1::SWE1* (untagged; this is not relevant to the experiment of Fig. 7, which was carried out in dextrose-containing media). To tag the *GAP::SWE1* construct, we used a de-

1. *Abbreviations used in this paper*: DAPI, 4′6′-diamidino-2-phenylindole; Lat-A, latrunculin-A.

Table I. Yeast Strains

Strain	Relevant genotype
DLY1	MATa *bar1*
DLY1028	MATa *swe1::LEU2 bar1*
JMY1233	MATa/α *cap2::URA3/CAP2 swe1::LEU2/SWE1*
JMY1169	MATa/α *tpm1::URA3/TPM1 swe1::LEU2/swe1::LEU2*
JMY1188	MATa/α *tpm1::URA3/TPM1*
JMY1216	MATa/α *sac6::URA3/SAC6 swe1::LEU2/swe1::LEU2*
JMY1215	MATa/α *sac6::URA3/SAC6*
JMY1196	MATa/α *pfy1-111:LEU2/pfy1-111:LEU2 swe1::LEU2/SWE1*
JMY2-24	MATa *myo2-66 swe1::LEU2*
JMY2-26	MATa *myo2-66*
JMY1280	MATa *cdc15-2*
JMY1281	MATa *cdc15-2 GAP:SWE1::HIS2*
JMY1341	MATa *bar1 GAL1::MIH1::TRP1*
JMY1342	MATa *bar1 tpm1::URA3 GAL1::MIH1::TRP1*
DLY2660	MATa *bar1 GAP::SWE1::HIS2*
JMY1292	MATa *bar1 mih1::LEU2*
RSY206	MATa *bar1 SWE1-myc::URA3::GAL1::SWE1*
RSY255	MATa *swe1::LEU2 GAP::SWE1-myc::HIS2::URA3*
RSY311	MATa *SWE1-myc::URA3*

rivative of the plasmid above, deleted for sequences between the XbaI and ClaI, lacking the GAL promoter and NH_2-terminal two thirds of *SWE1*. This was digested with KpnI and integrated into a *swe1Δ GAP::SWE1* strain. The resulting strain (RSY255) contains a single copy of *GAP::SWE1-myc* and an adjacent truncated promoterless *SWE1* fragment. The same strategy was used to make the *SWE1-myc* allele in strain RSY311, except the above KpnI-digested plasmid was transformed into a strain containing only the wild-type allele of *SWE1*. RSY311 contains a single copy of *SWE1-myc* and an adjacent truncated promoterless *SWE1*.

A plasmid containing *GAL1::MIH1*, pJM1016, was isolated from a GAL1::cDNA library (Liu et al., 1992). This clone contains the entire coding region of *MIH1* as well as seven bases upstream of the *MIH1* start codon. A KpnI/PstI fragment from pJM1016 containing the GAL1 promoter and the first 0.76 kb of *MIH1* were ligated into the KpnI/PstI site of the *TRP1* integrating vector pRS304 (Sikorski and Hieter, 1989), creating pJM1022. pJM1022 was digested with BglII (internal to *MIH1*) and transformed into yeast. Integration at the genomic *MIH1* locus generates a full-length *MIH1* under control of the *GAL1* promoter and an adjacent truncated *mih1* (3′ deleted). Integration was confirmed phenotypically by crossing to a *GAL1::SWE1* strain. *GAL1::MIH1* rescues the lethality of a *GAL1::SWE1* strain grown on galactose media.

Cells were grown in rich medium (YEPD: 1% yeast extract, 2% bactopeptone, 2% dextrose, 0.01% adenine) at 30°C, except where indicated. For pheromone arrest/release experiments, exponentially growing cells ($2–5 \times 10^6$ cells/ml) in YEPD were incubated with 20–25 ng/ml α-factor for 2 h, harvested by centrifugation, washed once with YEPD, and resuspended in fresh YEPD to release from the α-factor–induced cell cycle block. *bar1* strains were used in all of the α-factor synchrony experiments except for the *myo2-66* strains in Fig. 3 *A*, which are *BAR1* and were synchronized with 2 μg/ml α-factor.

Yeast Lysates and Immunoblotting

Yeast cells were washed with ice-cold H_2O and harvested by centrifugation. Pellets were stored frozen at −80°C. Lysates were made by resuspending pellets in a buffer containing 50 mM Tris-HCl, pH 7.5, 150 mM NaCl, 5 mM EDTA, 1% NP-40, 1 mM sodium pyrophosphate, 1 mM PMSF, 1 mM sodium orthovanadate, and 2 μg/ml each of aprotinin, pepstatin A, and leupeptin, and vortexing with acid-washed glass beads. Lysates were clarified by centrifugation (8 min, 14,000 rpm in an Eppendorf centrifuge [Madison, WI]), and the protein concentration was determined by the Bio-Rad assay (Hercules, CA). 50 μg of total protein (per gel lane) from each lysate was mixed with hot (95°C) 2× sample loading buffer (final concentrations 62.5 mM Tris-HCl, pH 6.8, 1% SDS, 25% glycerol, 355 mM β-mercaptoethanol, and 0.01% bromophenol blue) and incubated at 95°C for 5 min before running on a 10% polyacrylamide gel. After standard SDS-PAGE, proteins were transferred to immobilon transfer membrane (Millipore Corp., Bedford, MA), and the membrane was cut in two. The upper half was immunoblotted with anti-myc antibody and the bottom half with anti-PSTAIRE antibody (this recognizes Cdc28p and Pho85p). Membranes were first blocked in 5% dry milk in PBS with 0.1% Tween (PBS/Tween). Primary antibodies were used at 1:1,000 dilution (anti-myc) or 1:25,000 dilution (anti-PSTAIRE) in 1% milk/PBS-Tween. Secondary antibody was used at 1:2,500 dilution in PBS/Tween. All incubations were carried out for 1 h and separated by three washes with PBS/Tween. Blots were developed using the Renaissance Western Blot Chemiluminescence Reagent Plus (NEN™ Life Sciences Products, Boston, MA).

For the quantitative immunoblots in Fig. 8 *C*, asynchronous cultures of strains containing myc-tagged Swe1p expressed from its own promoter (RSY311, *top*) or the *GAP* promoter (RSY255, *middle*), as well as a control with no tagged Swe1p (DLY1, *bottom*), were lysed, and the indicated amounts of lysate were spotted onto nitrocellulose and processed for immunoblotting with anti-myc or anti-PSTAIRE (loading control) antibodies. The ratio of myc to PSTAIRE signal was quantitated by scanning densitometry using a Molecular Dynamics Personal Densitometer SI (Sunnyvale, CA) and ImageQuant v1.2 software.

Fluorescence Staining and Microscopy

DNA was visualized by staining with DAPI. Cells were fixed by the addition of two volumes of 95% EtOH directly to the yeast culture, followed by incubation for 30 min at room temperature or >12 h at 4°C. Cells were harvested by centrifugation and resuspended in 0.4 μg/ml DAPI in H_2O. F-actin was visualized by staining with rhodamine-conjugated phalloidin. Cells were fixed in ice-cold 70% EtOH for 15 min, harvested, washed, and resuspended in 20 U/ml rhodamine-conjugated phalloidin in PBS. The cells were then incubated for 30 min at room temperature, harvested, and washed three times with PBS. After the final wash, cells were resuspended in mounting media. Stained cells were viewed on a microscope (model Axioscope; Carl Zeiss, Inc., Thornwood, NY) equipped with epifluorescent and Nomarski optics. Images were captured using a Pentamax cooled CCD camera (Princeton Instruments, Princeton, NJ).

Spot Assays

To compare the growth of different strains, cells were sonicated and counted on a hemacytometer. For each strain, four 2-μl spots were pipetted onto a YEPD plate, each spot containing a total of ~1,250, 250, 50, or 10 cells, respectively. Strains being compared were pipetted onto the same plate. We found that many of our strains accumulated spontaneous suppressor mutations at quite high rates. It may be that any mutation that slows cell cycle progression would constitute a "suppressor" of a strain in which insufficient time is allowed for bud formation before mitosis; such suppressors might arise quite frequently and be strongly selected for in our strains. In an attempt to avoid this problem, heterozygous diploid strains were sporulated and dissected. Cells from haploid colonies were picked directly from the dissection plates and spotted as above, minimizing the selection of spontaneous "fast-growing" mutants. The temperature-sensitive *myo2-66* and *myo2-66 swe1::LEU2* strains, which can be maintained at the permissive temperature of 23°C, were the only exception to this strategy. Pictures of the plates were taken 2–3 d after spotting of the cells.

cap2::URA3 and *cap2::URA3 swe1::LEU2* strains were obtained from the sporulation of the diploid strain JMY1233. *tpm1::URA3* strains were obtained from the sporulation of JMY1188, and *tpm1::URA3 swe1::LEU2* were obtained from the diploid JMY1169. *sac6::URA3* and *sac6::URA3 swe1::LEU2* were spore isolates of JMY1215 and JMY1216, respectively, and the haploids *pfy1-111:LEU2* and *pfy1-111:LEU2 swe1::LEU2* were isolated from the sporulation of JMY1196.

Viability Assays

Synchronized cells were sonicated to disperse clumps and released into Lat-A–containing medium for the experiment in Fig. 4. At 1-h intervals, 5 μl of cells from each culture were diluted into 5 ml of fresh YEPD, and 100 μl of the diluted cells were plated onto YEPD plates. Triplicate dilutions were performed for each sample. The plates were incubated at 30°C for 2 d, and the number of colonies was counted. The average ± standard deviation was calculated for each triplicate set and is plotted as a percentage of the number of colonies on the $t = 0$ plates. Error bars indicate standard deviation. (Where no error bars are seen, the standard deviation was smaller than the size of the symbols used in the plot.)

Treatment of Cells with Lat-A

For Lat-A halo assays, 10^6 cells were spread onto a YEPD plate, and 2 μl of a 20 mM Lat-A stock solution in DMSO was pipetted onto the center of the plate. Cells were incubated at 30°C for 1 d, and the diameter of the halo was measured. For cells growing in liquid culture, Lat-A was added directly to the culture to the desired final concentration.

Results

A Swe1p-dependent Cell Cycle Delay in Cells with a Compromised Actin Cytoskeleton

Several mutants in actin cytoskeletal components have been identified that cause defects in actin organization but are not sufficiently severe to block bud formation. These include disruption of *CAP2*, encoding actin capping protein (Amatruda et al., 1990, 1992); *TPM1*, encoding tropomyosin (Liu and Bretscher, 1989, 1992); *SAC6*, encoding fimbrin (Adams et al., 1991); point mutation of *PFY1*, encoding profilin (Haarer et al., 1990, 1993); and *MYO2*, encoding type V myosin (Johnston et al., 1991). In general, these mutants grow slowly relative to wild-type cells but display good cell viability. We reasoned that the morphogenesis checkpoint might be delaying cell cycle progression in these mutants to compensate for the impairment in bud formation. If this is so, then elimination of checkpoint function in these cells should uncouple cell cycle progression from bud formation, leading to a reduction in viability.

To determine whether this was the case, we generated double mutants between *swe1Δ* and the actin cytoskeletal mutants and examined the growth of double versus single mutants (Fig. 2). Swe1p is essential for the operation of the morphogenesis checkpoint, but it has not been found to play any role in the unperturbed yeast cell cycle: under standard laboratory growth conditions, *swe1Δ* cells grow at the same rate as their wild-type counterparts and show a similar cell cycle profile (Fig. 2 *A*) (Booher et al., 1993; Sia et al., 1996). Therefore, any effects of Swe1p removal likely reflect the action of the checkpoint.

Four of the mutants examined (*tpm1Δ*, *sac6Δ*, *pfy1-111*, and *myo2-66*) displayed a clear reduction in viability when the morphogenesis checkpoint was crippled by elimination of Swe1p (Fig. 2 *B*). This strongly suggests that the actin perturbations caused by the mutants triggered the checkpoint response, as confirmed below.

Intriguingly, the degree of growth benefit provided by Swe1p varied depending on the growth temperature, in a mutant-specific manner. The difference between the growth of different mutants in combination with *swe1Δ* was most extreme at the temperatures shown in Fig. 2 *B* but was often reduced at other (7°C higher or lower) temperatures. In the most dramatic example, growth of *myo2-66 swe1Δ* cells was impaired relative to *myo2-66* cells at 29°C, but not at 28°C (Fig. 2 *B*). This was unexpected because the strain grows slowly and has impaired actin organization at both temperatures. One problem in interpreting growth assays for very sick strains is the accumulation of suppressor mutations. We attempted to avoid this problem by picking fresh colonies from tetrad dissection plates (see Materials and Methods) as the starting cells for the spot assays shown in Fig. 2 *B*, but we cannot rule out the possibility that suppressors were present in some of our assays, leading to the greater apparent health of the double mutants at some temperatures. However, these data suggest that the checkpoint is not capable of protecting the mutants at all temperatures, a point we will return to in the Discussion.

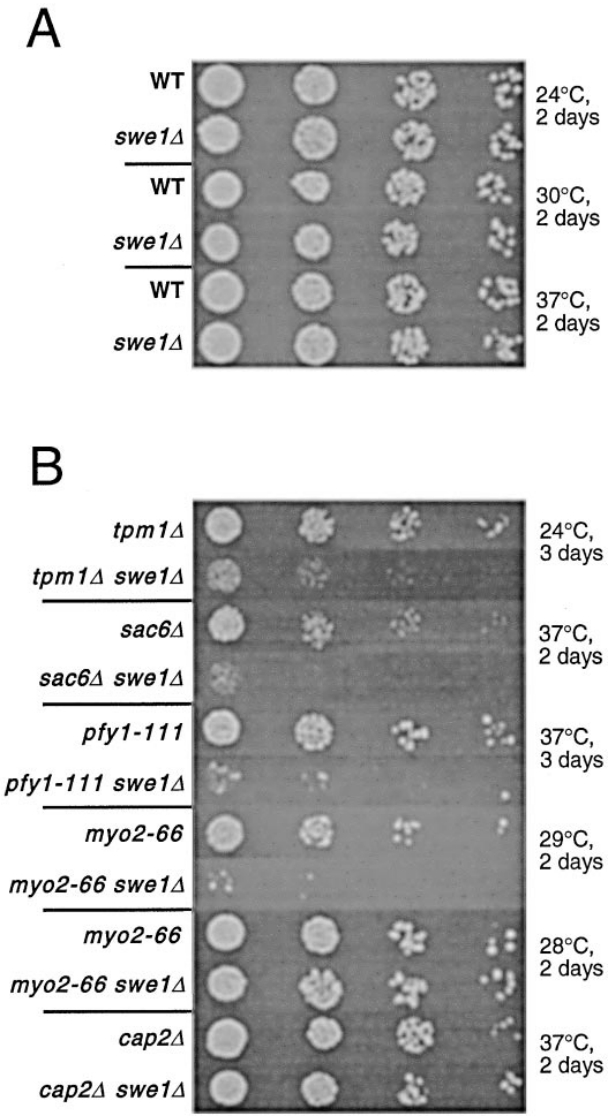

Figure 2. Requirement for Swe1p in cells with a compromised actin cytoskeleton. (*A*) Spot assays of wild-type (DLY1) and *swe1::LEU2* (DLY1028) cells at the indicated temperatures. No difference in the growth rate of the two strains was observed at any of the temperatures tested. (*B*) Spot assays of the indicated mutants. Each pair of strains (*SWE1* vs. *swe1::LEU2*) was compared on the same plate, but different pairs were incubated for different times at several temperatures, as indicated, and cannot be directly compared with each other. A one degree difference in temperature has a dramatic effect on the importance of Swe1p in temperature-sensitive *myo2-66* cells, although growth defects are observed in the *myo2-66* strain at both 28 and 29°C.

The *cap2Δ* mutation did not cause a marked growth defect at any temperature tested in our strain background, suggesting that bud formation was not slowed sufficiently to create a requirement for the checkpoint in this strain (Fig. 2 *B*).

The simplest interpretation of these results is that defects in actin cytoskeletal organization result in activation of the morphogenesis checkpoint, which aids the growth of the mutants by delaying mitosis until a suitable bud has been formed. To test this, we monitored cell cycle kinetics in synchronized mutant strains (Fig. 3). *myo2-66* and *myo2-66 swe1Δ* strains were arrested in G1 using α-factor at 23°C and then released at 30°C (the restrictive temperature, at which bud formation was blocked). As shown in Fig. 3 *A*, *myo2-66* cells displayed a delay in nuclear division relative to *myo2-66 swe1Δ* cells. We could not apply the same protocol to the other mutants because it was not possible to culture the *swe1Δ* double mutants without rapidly accumulating suppressor mutations. To circumvent this problem, we integrated a *GAL1::MIH1* construct into wild-type and *tpm1Δ* mutant strains. This construct directs overexpression of Mih1p (the phosphatase that reverses the Cdc28p phosphorylation catalyzed by Swe1p; Russell et al., 1989) in cells grown on galactose medium, but not in cells grown on dextrose or sucrose as carbon source. Thus, we could conditionally counteract Swe1p activity by culturing the cells on galactose. Cells were grown in sucrose media, synchronized in G1 with α-factor at 30°C, and released into dextrose- or galactose-containing media (Fig. 3 *B*). The *tpm1Δ* strain displayed a distinct delay of bud formation relative to the wild-type control, in both dextrose and galactose media, as expected. While on dextrose, *tpm1Δ* cells also delayed nuclear division (Fig. 3 *B*, compare *top two panels*), on galactose this delay was eliminated (Fig. 3 *B*, compare *bottom two panels*). The resulting rapid nuclear division in cells that were compromised for bud formation led to the accumulation of unbudded binucleate cells (Fig. 3 *C*). Thus, *myo2-66* and *tpm1Δ* mutants experienced a cell cycle delay resulting from Cdc28p tyrosine phosphorylation (reversible by Swe1p elimination or Mih1p overexpression). Together with the results from Fig. 2, these data suggest that perturbation of actin organization triggers the morphogenesis checkpoint to produce a Swe1p-dependent delay of the cell cycle, which provides time for cells to form a bud before undergoing nuclear division.

Lat-A Triggers a Swe1p-dependent Delay of Nuclear Division

The drug Lat-A binds to monomeric actin and prevents actin polymerization (Ayscough et al., 1997). Drubin and co-workers have recently shown that Lat-A inhibits yeast growth in a concentration-dependent manner (Ayscough et al., 1997). Selected mutations in the *ACT1* gene, encoding actin, confer Lat-A resistance, confirming that growth inhibition is due to actin perturbation (Ayscough et al., 1997). Treatment of yeast cells with 0.1 mM Lat-A results in rapid (5–10 min) and complete depolymerization of F-actin (Fig. 4 *A* and Ayscough et al., 1997). We synchronized wild-type and *swe1Δ* cells in G1 using α-factor and

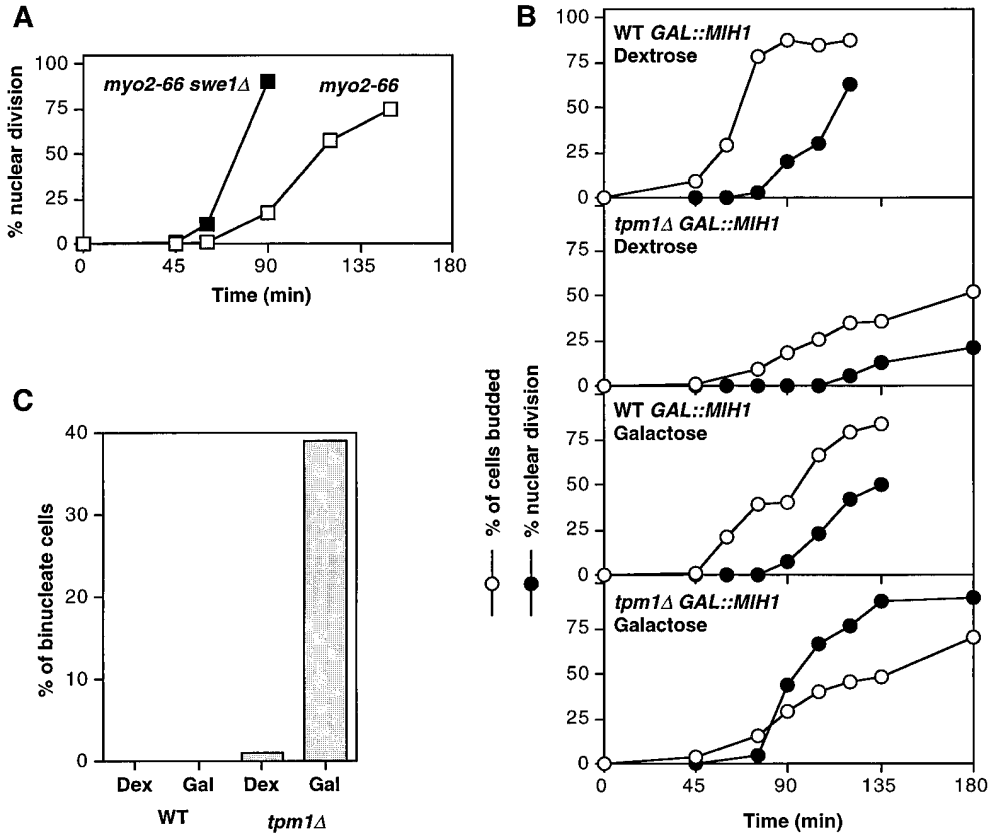

Figure 3. Checkpoint-induced delay of nuclear division in *myo2-66* and *tpm1Δ* mutants. (*A*) Kinetics of nuclear division in *myo2-66* (JMY2-26) and *myo2-66 swe1::LEU2* (JMY2-24) cells synchronized in G1 with α-factor at 23°C and released into fresh YEPD at 30°C. (*B*) Wild-type (JMY1341) and *tpm1Δ* (JMY1342) strains containing the inducible *GAL1::MIH1* construct were grown in YEPS (sucrose-containing) media at 30°C and arrested with α-factor for 2.5 h. Dextrose (*top two panels*) or galactose (*bottom two panels*) was added to a final concentration of 2%, and the incubation was continued for a further 1.5 h. At this point, the cells were homogeneously arrested in G1 and did (galactose) or did not (dextrose) overexpress Mih1p. Cells were harvested by centrifugation and resuspended in fresh YEPD (*top panels*) or YEPG (galactose; *bottom panels*) at 30°C. The kinetics of bud formation (*open circles*) or nuclear division (*closed circles*) were determined at different times. (*C*) The percentage of cells that became binucleate without forming a bud is shown for the same cells in *B*, at the 2-h time point.

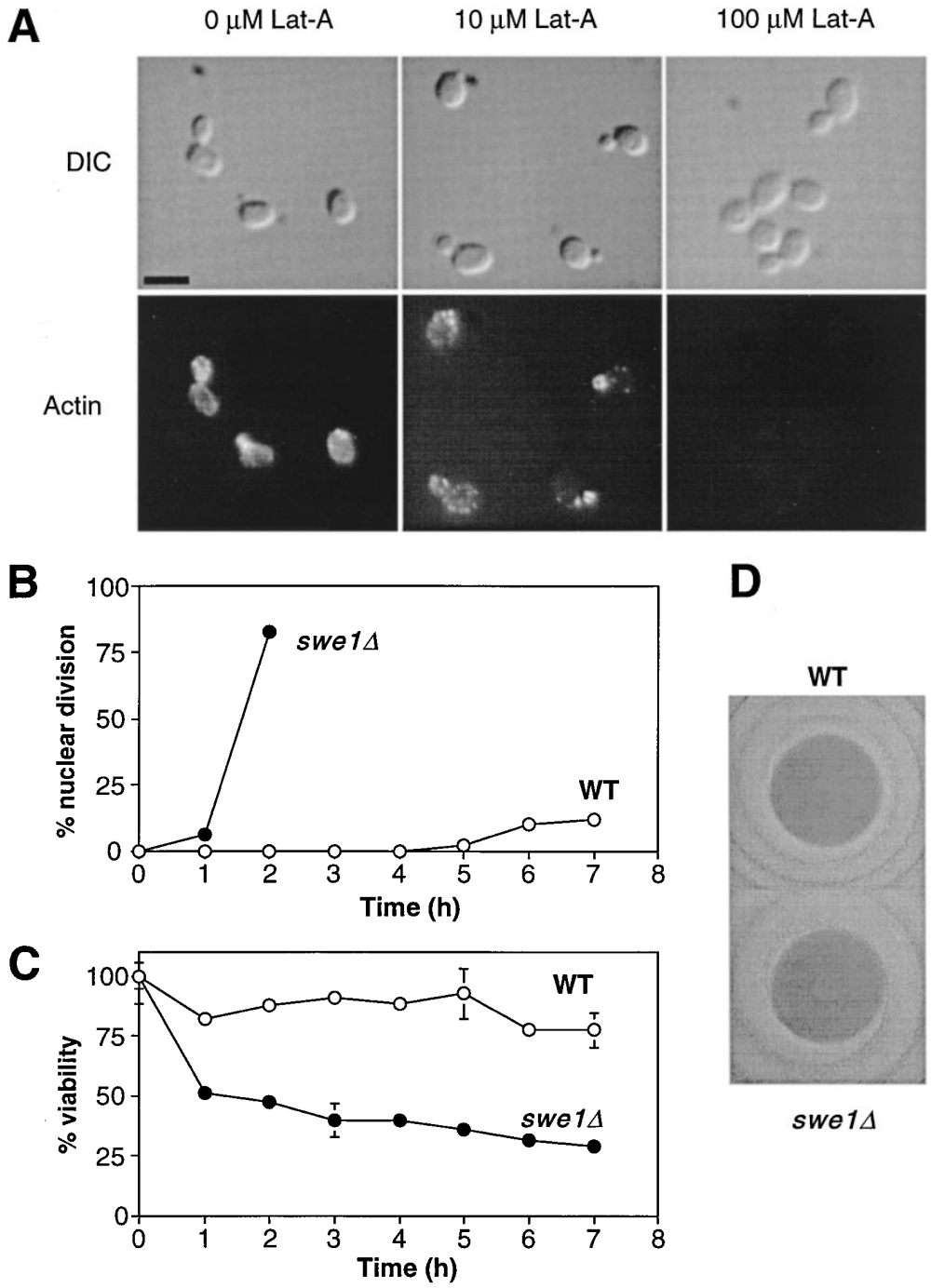

Figure 4. Swe1p-dependent cell cycle arrest in Lat-A–treated cells. (*A*) F-actin organization in cells exposed to Lat-A. Exponentially growing wild-type (DLY1) cells were exposed to 0, 10, or 100 μM Lat-A for 1 h at 30°C and then fixed and stained with rhodamine-phalloidin. No actin structures were seen in cells treated with 100 μM Lat-A (equal exposures are shown for all fluorescence panels). Cortical actin patches were readily detected in cells treated with 10 μM Lat-A and were frequently polarized towards the presumptive bud site in unbudded cells and the tip of the bud in small-budded cells, but no cables were seen. (*B*) Kinetics of nuclear division for wild-type (DLY1) and *swe1Δ* (DLY1028) cells after release from α-factor–induced G1 arrest into fresh media containing 100 μM Lat-A. (*C*) Viability of the same cells in *B*. Viability was assayed by the ability of the cells to give rise to colonies once the Lat-A was washed out, as described in Materials and Methods. (*D*) Lat-A halo assay. 2 μl of 20 mM Lat-A was spotted onto YEPD plates spread with wild-type (DLY1) or *swe1::LEU2* (DLY1028) cells. The diameter of the zone of no growth, or "halo," was 12 mm for both strains. Bar, 5 μm.

then washed out the α-factor and added 0.1 mM Lat-A (Fig. 4 *B*). Flow cytometric analysis demonstrated that DNA replication was complete by 60 min in both strains (data not shown). However, microscopic analysis revealed that wild-type cells treated with Lat-A did not undergo nuclear division for the entire 7-h time course of the experiment (Fig. 4 *B*). This block to nuclear division was Swe1p dependent because *swe1Δ* cells completed nuclear division by 2 h (Fig. 4 *B*). Thus, like the actin-perturbing mutants, Lat-A treatment triggers the morphogenesis checkpoint.

SWE1 Protects Cells from Transient Exposure to Lat-A

To assess whether the Swe1p-mediated cell cycle arrest was effective in maintaining cell viability during Lat-A treatment, cells from the same experiment as Fig. 4 *B* were assayed for viability (i.e., the ability to form colonies) after different times of exposure to Lat-A (Fig. 4 *C*). The results in this experiment show that wild-type cells retained good viability (>75%) even after 7 h of Lat-A treatment. In contrast, 50% of the *swe1Δ* mutant cells lost the ability to form colonies after only 1 h in Lat-A (Fig. 4 *C*). This timing may seem surprisingly rapid since *swe1Δ* cells underwent nuclear division between 1 and 2 h after release from pheromone arrest. However, we have confirmed the observation of Ayscough et al. (1997) that actin structures are not recovered immediately upon Lat-A removal, but rather take ~1 h to reform and become polarized. Thus, 1 h

of Lat-A exposure corresponds to closer to 2 h of absent or disorganized F-actin, by which time the *swe1Δ* cells had completed nuclear division.

Although 50% of the *swe1Δ* cells lost viability rapidly in this experiment, the remaining cells were apparently able to withstand prolonged exposure to Lat-A, with only a gradual loss of viability (Fig. 4 *C*). We are currently mystified by this heterogeneity in the response of the *swe1Δ* population to Lat-A and cannot explain why some cells live while others die rapidly. However, it is worth bearing in mind that the viability assay we used monitors the ability of cells to give rise to colonies in a very nutrient-rich environment and in isolation from other cells. It seems likely that if wild-type and *swe1Δ* cells were mixed in a competitive environment, a large majority of the *swe1Δ* cells would be at a severe disadvantage after even a brief Lat-A exposure.

During the course of these studies, we discovered that cells arrested using higher doses of pheromone (100 ng/ml versus the 20 ng/ml used in Fig. 4; note that all strains are *bar1Δ*) were very slow to recover from the G1 arrest. (Data not shown; we speculate that the Lat-A prevents endocytosis of pheromone-bound receptors and hence recovery from pheromone arrest.) Under these circumstances, wild-type and *swe1Δ* cells retained viability to a similar extent (data not shown). This suggests that the viability loss observed for *swe1Δ* cells in Fig. 4 *C* is a consequence of continued cell cycle progression and does not reflect some other role for Swe1p.

SWE1 Does Not Protect Cells from Continuous Exposure to Low Doses of Lat-A

The sensitivity of yeast strains to Lat-A is easily measured using a "halo" assay, in which a spot of concentrated Lat-A is placed in the middle of a lawn of yeast cells. The drug diffuses out from this spot and creates a halo, or zone of growth inhibition, in which cells cannot proliferate; the size of the halo reflects the sensitivity of the strain to Lat-A (Ayscough et al., 1997). To test whether the morphogenesis checkpoint would allow wild-type cells to withstand a greater degree of continuous actin perturbation, we performed Lat-A halo assays on isogenic wild-type and *swe1Δ* strains. At the concentration of Lat-A present at the edge of the halo, bud formation is presumably delayed but not blocked; at these doses, the checkpoint would be expected to maintain coordination between the impaired bud formation and cell cycle progression, permitting cell proliferation. If this were the case, *swe1Δ* cells would be unable to maintain that coordination and should therefore display a larger halo. Unexpectedly, the size of the halo was identical for the two strains (Fig. 4 *D*), showing that Swe1p does not protect cells from continuous exposure to low doses of Lat-A.

The Checkpoint Delay of Nuclear Division Is Not Commensurate with the Delay of Bud Formation at Low Doses of Lat-A

Why does the checkpoint-induced G2 delay not help cells to survive continuous exposure to Lat-A? To address this question we repeated the synchrony experiment using lower doses of Lat-A (Fig. 5). At these concentrations, cells retained the ability to polymerize and (at the lower doses) to polarize actin (Fig. 4 *A*), and bud formation was delayed to varying extents (Fig. 5 *A*). As expected, Lat-A–treated cells displayed a delay in nuclear division compared with untreated cells, and the duration of the delay increased with the dose of Lat-A (Fig. 5). Surprisingly, however, the delay of nuclear division was not commensurate with the delay of bud formation. As the dose of Lat-A was increased, the time between bud formation and nuclear division decreased, until the events were reversed and cells became binucleate before they could form a visible bud (see Fig. 5 *B*, *top*). Presumably, this explains why the checkpoint fails to protect cells from low doses of Lat-A: even with an active checkpoint, the cell cycle is insufficiently delayed to cope with the delay in bud formation.

As expected, the delay of nuclear division was Swe1p dependent at all doses of Lat-A (Fig. 5 *B*, *middle*). One consequence of this was that low doses of Lat-A, which still permitted bud formation in wild-type cells, were sufficient to block bud formation in *swe1Δ* cells (Fig. 5 *B*, compare *top two panels*). Previous work has established that the cyclin/Cdc28p complexes that promote mitosis also promote actin depolarization during the cell cycle; inhibition of these complexes by Swe1p maintains a cyclin/Cdc28p configuration that promotes actin polarization (Lew and Reed, 1993). Thus, in wild-type cells exposed to low doses of Lat-A, Swe1p delays the cell cycle at a stage when cyclin/Cdc28p complexes promote actin polarization, and given sufficient time, the actin cytoskeleton can polarize and build a bud. In *swe1Δ* cells, the actin cytoskeleton is similarly competent to build a bud but is not given sufficient time to do so before the cell cycle progresses to a point when cyclin/Cdc28p complexes now promote actin depolarization, and bud formation does not occur.

The duration of the cell cycle delay in Lat-A was determined by Mih1p (Fig. 5 *B*, *bottom*). In *mih1Δ* cells, equivalent doses of Lat-A caused greatly prolonged delays of nuclear division compared with wild-type cells, and the delay between bud formation and nuclear division increased with Lat-A dose, rather than decreasing as in the wild type. This shows that Mih1p terminates the cell cycle delay in wild-type cells exposed to Lat-A, and that termination is not dependent on bud formation. As discussed below, this finding is inconsistent with a model in which the checkpoint simply delays nuclear division until a bud has been formed.

Lat-A Can Arrest Nuclear Division in Cells That Have Already Formed a Bud

In the synchrony experiments described above, the checkpoint was triggered by perturbation of actin in unbudded cells. Thus, bud formation was itself delayed or inhibited, and it was not clear from these experiments whether the actin perturbation itself or the consequent delay of bud formation was responsible for triggering the checkpoint. To distinguish between these options, we wished to determine whether actin perturbation would trigger the checkpoint in cells that had already formed a bud. To test this, we treated asynchronous wild-type and *swe1Δ* populations with 0.2 mM Lat-A for 3 h (approximately two doubling times for unperturbed cells at 30°C). As expected, the un-

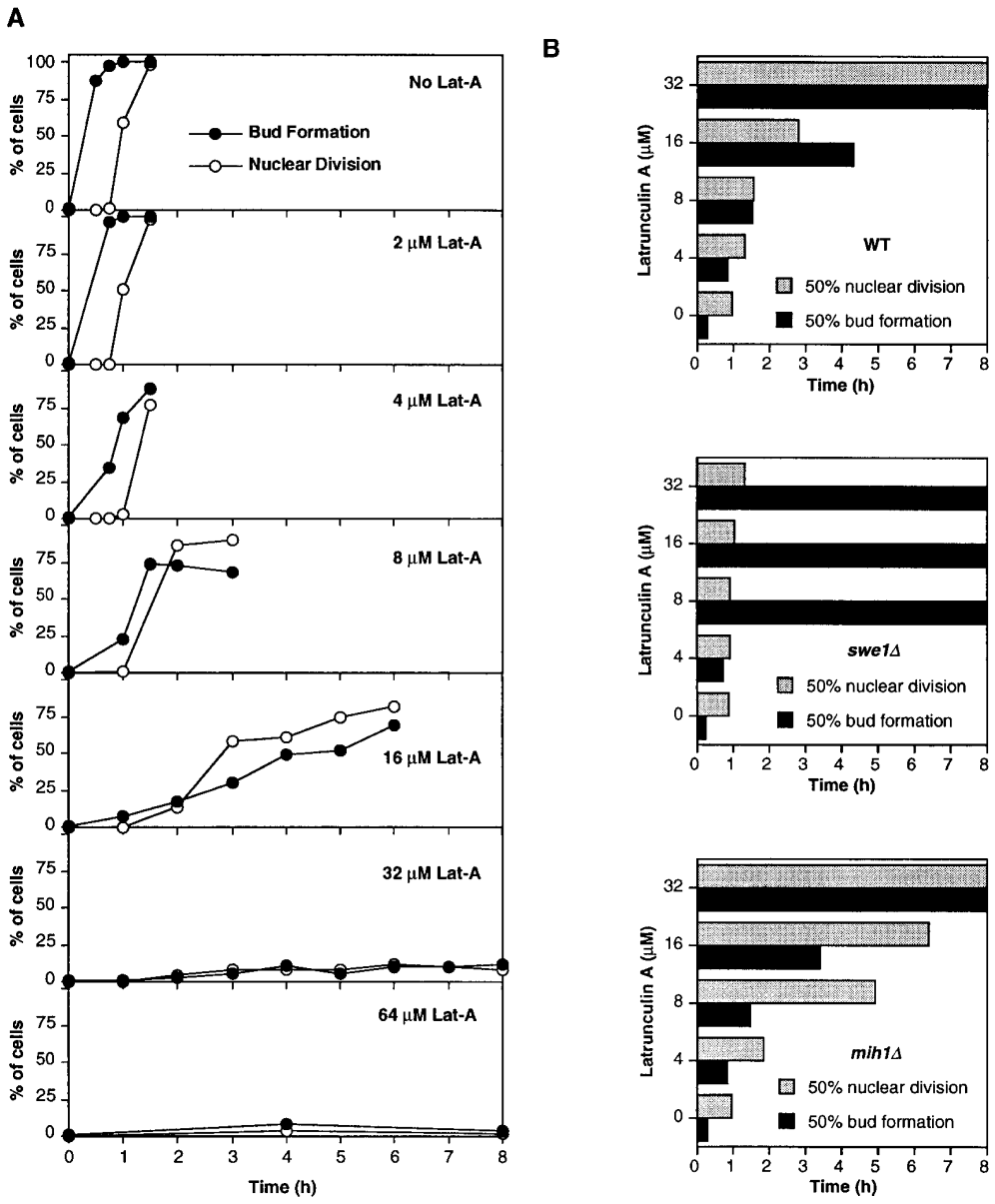

Figure 5. The checkpoint delay at low doses of Lat-A. (*A*) Kinetics of bud formation and nuclear division in wild-type cells (DLY1) after release from α-factor–induced G1 arrest into fresh media containing the indicated concentrations of Lat-A. (*B*) (*Top*) The data from *A* is replotted as the time taken for 50% of the cells to form buds (*black bars*) or undergo nuclear division (*gray bars*) at the indicated concentrations of Lat-A. The middle and bottom panels represent similar plots from identical experiments with *swe1::LEU2* (DLY1028, *middle*) and *mih1:LEU2* (JMY1292, *bottom*) strains.

budded cells in the wild-type population did not undergo nuclear division, while many of the *swe1Δ* cells did (Fig. 6 *A*). Budded wild-type cells displayed a mixed response: 56% contained two nuclei, while 44% contained a single nucleus (Fig. 6 *A*). In general, cells with single nuclei had small buds, while cells with two nuclei had larger buds. In contrast, almost all of the budded *swe1Δ* cells contained two nuclei (Fig. 6 *A*). This experiment demonstrates that the checkpoint can respond to actin perturbation even after cells have formed a bud.

Some of the cells in this experiment underwent cytokinesis during the 3 h time course (Fig. 6 *A*), making it difficult to determine the size of the subset of budded cells that actually arrested before anaphase upon Lat-A treatment. To circumvent this problem, we introduced the *cdc15-2* mutation into the strain background. At the restrictive temperature, this mutation prevents cytokinesis (Pringle and Hartwell, 1981), which allowed us to accurately quantitate the proportion of cells that underwent nuclear division after Lat-A addition (Fig. 6 *B*, *left*). Asynchronous populations of *cdc15-2* cells were grown at 24°C and shifted to 37°C. Lat-A was added to 0.2 mM 10 min after the temperature shift, and the cells were incubated for a further 3 h. Under these conditions, unbudded cells could not form a bud (because of the Lat-A), and budded cells could not undergo cytokinesis (because of the *cdc15-2* mutation). Unbudded cells arrested with a single nucleus, as expected. Of the budded cells, 34% of the pre-anaphase cells arrested with a single nucleus (Fig. 6 *B*). Thus, the ability to respond to actin perturbation is not maintained throughout the budded portion of the cell cycle: only about one third of the budded cells (probably representing the cells with the smallest buds; see below) underwent a Swe1p-dependent G2 arrest upon Lat-A addition.

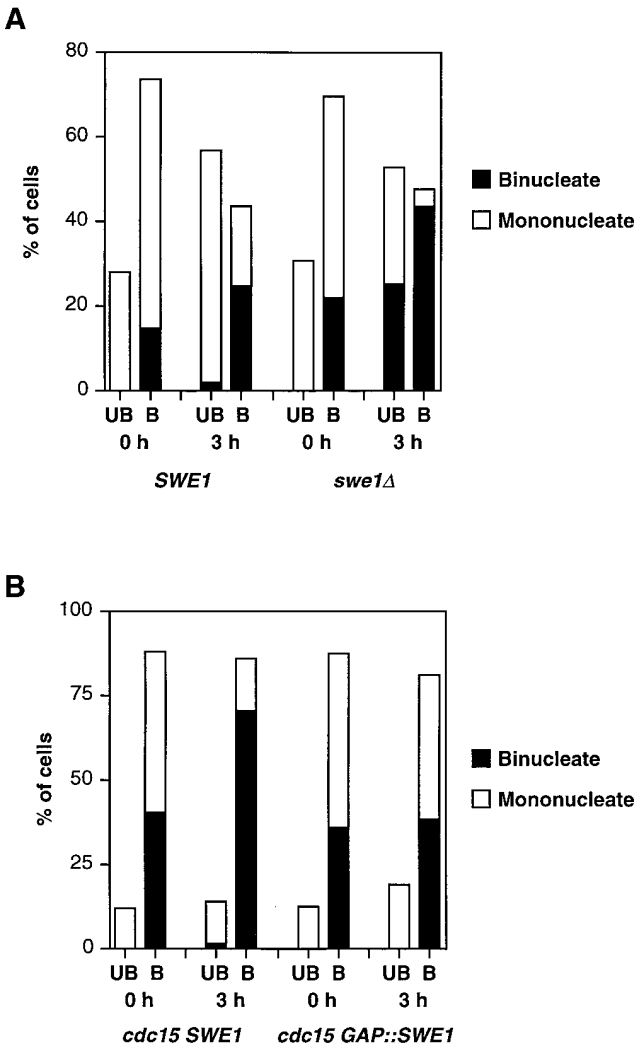

Figure 6. Budded cells can respond to Lat-A. (*A*) Wild-type (DLY1) and *swe1::LEU2* (JMY3-3) cells were exposed to 200 μM Lat-A for 3 h at 30°C. The percentage of unbudded (*UB*) and budded (*B*) cells containing one nucleus (*white bars*) or two nuclei (*black bars*) were calculated before and after Lat-A treatment. The increase in the percentage of unbudded cells is due to cytokinesis of some of the budded cells, which subsequently arrest as unbudded cells. (*B*) Asynchronous populations of temperature-sensitive *cdc15* (JMY1280) and *cdc15 GAP::SWE1* (JMY1281) cells were treated as in *A*, except that cells were shifted to the nonpermissive temperature of 37°C 10 min before the addition of Lat-A to prevent cytokinesis (a phenotype of the *cdc15* allele).

Swe1p Accumulates Periodically during the Cell Cycle

Why do budded cells lose the capacity to arrest cell cycle progression in response to actin perturbation? One possibility is suggested by the observation that *SWE1* mRNA accumulates periodically during the cell cycle, with a peak in late G1 (Lim et al., 1996; Ma et al., 1996; Sia et al., 1996). If the presence of Swe1p were restricted to cells that were at an early stage of the cell cycle, then the population of cells that arrested in response to Lat-A may correspond to the subset of cells that contained Swe1p. Later in the cell cycle, there would be insufficient Swe1p to promote cell cycle arrest, even if the Lat-A were to trigger the upstream components of the checkpoint pathway. In this scenario, the checkpoint "detector" would detect the actin perturbation at any stage of the cell cycle, but would only cause cell cycle arrest in cells that contained the "receiver" of the checkpoint signal, Swe1p.

To determine whether Swe1p accumulation was indeed periodic during the cell cycle, we generated an epitope-tagged version of *SWE1*, *SWE1-myc*, integrated at the *SWE1* locus under the control of the *SWE1* promoter (see Materials and Methods). Control experiments indicated that this construct retained full activity (Sia, R.A.L., E.S.G. Bardes, and D.J. Lew, manuscript submitted for publication). The monoclonal 9E12 (anti-myc) antibody recognized a band of ~180 kD in cells expressing Swe1p-myc, but not in cells lacking the tagged construct (Fig. 7 *B*, *left two lanes*). Cells containing tagged Swe1p were synchronized using an α-factor arrest/release protocol, and the abundance of Swe1p was monitored by Western blotting through the cell cycle (Fig. 7). Swe1p accumulation

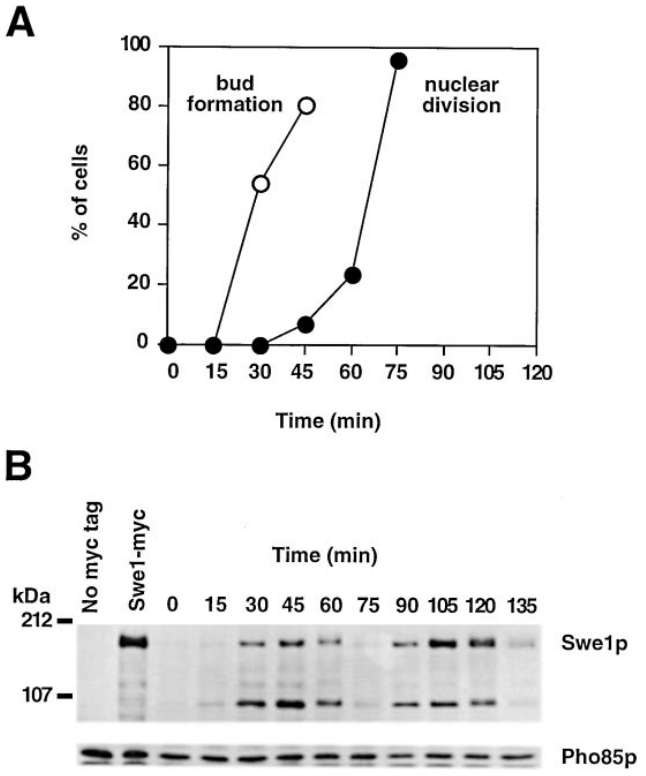

Figure 7. Swe1p accumulation is periodic during the cell cycle. (*B*) *Left two lanes*, lysates of asynchronous wild-type cells (DLY1, *No myc tag*) or cells containing an integrated *SWE1-myc12* (RSY206) were separated by SDS-PAGE and immunoblotted with the 9E10 monoclonal anti-myc antibody (*upper panel*) or a monoclonal anti-PSTAIRE antibody as a loading control (*lower panel*; two proteins are recognized by this antibody in yeast lysates—the upper band corresponds to Pho85p and the lower band to Cdc28p). *Right lanes*, similar immunoblots of the *SWE1-myc12* (RSY206) strain at the indicated time points after release from α-factor–induced G1 arrest into fresh media. The kinetics of bud formation and nuclear division for the first cell cycle in the same experiment are plotted in *A*.

was periodic during the cell cycle, rising at the time of bud emergence and declining again before nuclear division. This pattern of accumulation is consistent with the previously described pattern of *SWE1* transcriptional regulation and suggests that Swe1p is a moderately unstable protein.

Periodic Swe1p Expression Limits Checkpoint Action during the Cell Cycle

To determine whether the periodic expression of Swe1p was responsible for the decrease in checkpoint efficacy during the budded portion of the cell cycle, we generated a strain in which *SWE1* transcription was constitutive throughout the cell cycle by integrating three to four copies of a *GAP::SWE1* allele into a wild-type strain at the *HIS2* locus (Sia et al., 1996; note that although mRNA levels driven by this construct are constant through the cell cycle, posttranslational regulation of Swe1p might still occur). Quantitative immunoblotting of myc-tagged Swe1p driven by this construct (Fig. 8 *C*) in asynchronous cells suggests that it expresses only 30% as much Swe1p as the wild-type gene. Thus, three to four copies (in addition to the wild type) would lead to approximately twofold overexpression of Swe1p (comparing asynchronous populations). The doubling time and cell cycle profile of the *GAP::SWE1*-containing strain was indistinguishable from that of wild-type cells (Fig. 8 *A*), indicating that this degree of Swe1p overexpression was insufficient to delay nuclear division in unperturbed cells.

Wild-type and *GAP::SWE1*-containing strains were synchronized with α-factor and treated with Lat-A at different times after release from the arrest. In this experiment, bud formation occurred at 10–20 min, and nuclear division occurred at 40–50 min (Fig. 8 *A*). At the intervening times (20, 30, and 40 min) when cells had formed buds but not yet undergone nuclear division, aliquots of cells were treated with 0.1 mM Lat-A and subsequently fixed at 90 min. By this time, untreated cells had completed nuclear division (Fig. 8 *A*). However, a subset of the Lat-A–treated cells arrested without undergoing nuclear division (Fig. 8 *B*). In the wild-type cells, only 50% of budded cells arrested in response to Lat-A even at the 20 min stage when cells had formed small buds, and the proportion of responding cells decreased as cells progressed through the cell cycle (Fig. 8 *B*, *white bars*). In contrast, 99% of the budded *GAP::SWE1*-containing cells arrested in response to Lat-A at the 20 min stage (Fig. 8 *B*, *black bars*). Fewer cells responded at later times, but the fraction of responding cells remained much higher than in the wild type at all times. This experiment demonstrates that cells with larger buds can detect the actin perturbation caused by Lat-A and respond by arresting nuclear division if sufficient Swe1p is present. In wild-type cells, the ability to mount a response decreases shortly after bud formation because Swe1p levels decline.

We have confirmed these observations in asynchronous populations of *cdc15-2* cells expressing *GAP::SWE1* (Fig. 6 *B*, *right*). While only 34% of budded pre-anaphase cells expressing the wild-type *SWE1* arrested in response to Lat-A, 85% of the budded pre-anaphase cells expressing the constitutive *GAP::SWE1* arrested before nuclear division (Fig. 6 *B*). These experiments strongly suggest that

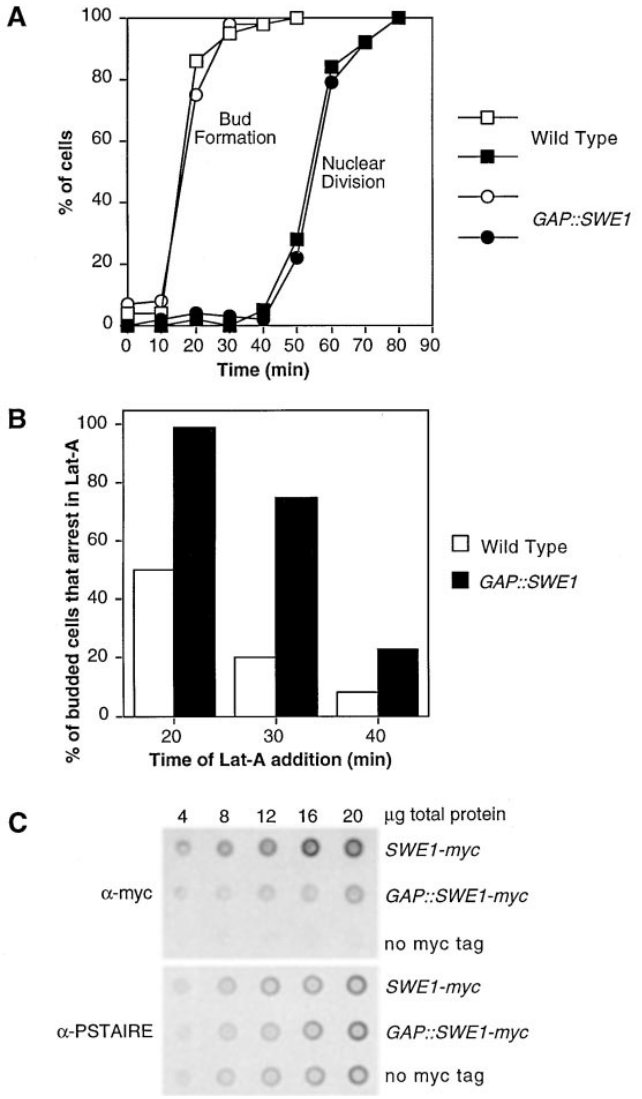

Figure 8. The checkpoint response in budded cells from strains expressing periodic or constitutive Swe1p. (*A*) Kinetics of bud formation and nuclear division in wild-type cells (DLY1, *squares*) and cells containing three to four copies (determined by Southern blots) of an integrated *GAP::SWE1* construct (DLY2660, *circles*) after release from α-factor–induced G1 arrest into fresh media. (*B*) At the indicated times of the synchrony experiment shown in *A*, 100 μM Lat-A was added to aliquots of the culture, and the incubation was continued until $t = 90$ min. The cells were fixed and stained to visualize nuclei, and the percentage of budded cells that remained mononucleate (i.e., were arrested in response to Lat-A) is plotted. *White bars*, wild-type cells; *black bars*, *GAP::SWE1* cells. (*C*) A strain containing a single myc-tagged *GAP::SWE1* expresses 30 ± 10% (standard deviation) as much Swe1p as a strain containing myc-tagged *SWE1* on its own promoter, as quantitated by scanning densitometry of the dot immunoblots shown (see Materials and Methods for details).

Lat-A can trigger a Swe1p-dependent G2 arrest through most of the cell cycle, provided that sufficient Swe1p is present.

Discussion

The experiments reported in this paper allow us to draw

three novel conclusions regarding the morphogenesis checkpoint in budding yeast. First, the checkpoint monitors defects at the level of actin organization. Our data cannot be accommodated by models in which the checkpoint simply monitors upstream polarity establishment functions or downstream events such as bud formation or bud growth. The possibility remains that the checkpoint might monitor multiple processes in addition to actin organization, although there is currently no need to invoke such complexity to explain the available data. Second, the checkpoint can detect perturbation of actin integrity at any stage of the cell cycle between Start and nuclear division. Third, the efficacy of the checkpoint in responding to actin perturbation by arresting cell cycle progression is limited to a critical window of the cell cycle (the time of initial bud emergence and growth) by the periodic expression of the checkpoint effector, Swe1p. As a consequence of these features, environmental insults that perturb actin organization will only delay nuclear division in cells that have not yet constructed a mature bud, and the effect of the checkpoint is to couple nuclear division to successful bud formation.

The Morphogenesis Checkpoint Responds to Perturbation of Actin Organization

We have previously shown that perturbation of cell polarity in yeast triggers a morphogenesis checkpoint that delays nuclear division (Lew and Reed, 1995*a*; Sia et al., 1996). In this report, we have investigated the effects of perturbing the actin cytoskeleton itself, rather than polarity establishment functions, on cell cycle progression. We found that both mutation of genes encoding actin-associated proteins and the actin-depolymerizing drug Lat-A produced a delay or arrest of the cell cycle before nuclear division. The cell cycle delay was dependent upon Swe1p, arguing that it was a consequence of the morphogenesis checkpoint. These findings have important implications for the structures that might be monitored by the checkpoint. Cells lacking F-actin altogether are still able to polarize Cdc42p, septins, and other cortical proteins (Ayscough et al., 1997). Thus, the fact that actin perturbations trigger the checkpoint suggests that the checkpoint does not simply monitor polarity establishment or septin assembly. More likely, the checkpoint monitors the actin cytoskeleton itself, or perhaps a process that is tightly linked to correct actin organization.

One process that depends on polarized actin is polarized secretion and/or cell wall deposition. Like the actin perturbations described here, mutation of *BED1* (also called *MNN10* and *SLC2*) created a requirement for the morphogenesis checkpoint (Mondesert and Reed, 1996). The *bed1* mutant impaired protein glycosylation and displayed a pronounced delay in bud formation (Dean and Poster, 1996; Mondesert and Reed, 1996). Defects in actin organization were apparent in one *bed1* strain, but actin was apparently normal in *bed1* mutants from another strain background (Karpova et al., 1993; Mondesert and Reed, 1996). Thus, it is unclear whether *bed1* mutants trigger the checkpoint through an effect (which can be quite subtle) on actin organization itself or through effects on a downstream process involving protein glycosylation. A similar uncertainty exists for the interpretation of other mutants affecting protein glycosylation and secretion that were isolated in the same genetic screen as *bed1* (Mondesert et al., 1997). However, these studies do support our conclusion that either actin organization itself or a process that depends on proper actin organization is monitored by the checkpoint.

The most obvious actin-dependent cell cycle events that the checkpoint could respond to are the emergence or growth of the bud. For instance, there may be some way to detect the presence of a bud (or perhaps a neck, which would be unique to budded cells) or to assess the size or maturity of a bud. If the checkpoint were to monitor bud emergence or bud size, then once a suitable bud had been formed, perturbation of actin would no longer be expected to have any effect on cell cycle progression. However, we found that in cells expressing a constitutive level of *SWE1* mRNA, actin perturbation was in fact able to halt cell cycle progression even when cells had successfully constructed a large bud. This demonstrates that the structure monitored by the checkpoint is still actin dependent after a large bud has been formed, arguing that the checkpoint does not simply monitor the presence or size of the bud.

Does the Checkpoint Monitor Completion of a Cell Cycle Event?

Complete actin depolymerization blocked cell cycle progression, while less severe actin perturbations produced G2 delays of various lengths. This raises the question of what determines the duration of the G2 delay in response to different perturbations. One possibility is that the duration of the delay simply reflects the time needed to complete an actin-dependent cell cycle event, which takes more or less time depending on the degree of perturbation. Termination of the checkpoint delay then occurs when the hypothetical event is complete. Although the delays in response to some perturbations (e.g., *tpm1Δ* mutants) were sufficient to permit bud formation, we found that in cells treated with some doses of Lat-A, the checkpoint delay was terminated before most cells could make a bud. Similarly, a complete block of cell polarity (imposed using temperature-sensitive *cdc24* or *cdc42* mutants) produces only a transient delay in nuclear division (Lew and Reed, 1995*a*; Sia et al., 1996). Thus, if termination of the delay reflects completion of some event, then that event can be completed in the absence of detectable polarity in unbudded cells. As mentioned above, actin perturbation can produce a delay even in cells with large buds. Thus, to accommodate our observations, the hypothetical actin-dependent event monitored by the checkpoint would have to occur very late in the unperturbed cell cycle but would be attainable even in unbudded cells. It is difficult to imagine an event that meets these criteria.

An alternative hypothesis is that instead of monitoring completion of a cell cycle event, the checkpoint continuously monitors the status of the actin cytoskeleton. Just as the DNA damage checkpoint continuously monitors DNA integrity rather than any particular cell cycle event, we propose that the morphogenesis checkpoint monitors the integrity or organization of the actin cytoskeleton. Because actin integrity is subject to perturbation at any stage

of the cell cycle, it is easy to incorporate the observation that actin perturbations can be detected in large-budded as well as unbudded or small-budded cells.

Duration of the Checkpoint Delay: The Role of Adaptation

If the checkpoint responds to disruption of cytoskeletal integrity, what terminates the checkpoint delay? Since nuclear division in mutants with disrupted cell polarity occurred with no apparent recovery of cell polarity, we proposed that the checkpoint displays adaptation (Sia et al., 1996). Adaptation has also been described for the DNA damage checkpoint (Sandell and Zakian, 1993; Toczyski et al., 1997). To accommodate the data reported here, we extend this idea by supposing that mild perturbation of actin organization leads to rapid adaptation, while more severe perturbations cause progressively slower adaptation. Both in the case of mutants disrupting cell polarity (Sia et al., 1996) and wild-type cells exposed to Lat-A (Fig. 5 *B*), termination of the checkpoint delay requires the phosphatase Mih1p.

The adaptation hypothesis does not link termination of the checkpoint delay to completion of a specific cell cycle event. This makes it much easier to explain why some perturbations apparently trigger appropriate delays (i.e., the cell cycle delay matches the delay in bud formation) while others (such as low doses of Lat-A) do not. In addition, the variable success of the checkpoint in terms of matching the cell cycle delay to the delay of budding may explain why the presence of Swe1p improved the viability of mutants with impaired actin organization at some, but not all, temperatures. Presumably, the checkpoint evolved to cope with physiological insults (such as temperature or osmolarity changes) that affect the cytoskeleton. The adaptation process would provide appropriate delays for those perturbations, but not necessarily for the artificial perturbations we have tested here.

Periodic SWE1 Transcription Limits Checkpoint Action during the Cell Cycle

Transcription of *SWE1* is periodic during the cell cycle, with a peak in late G1 (Lim et al., 1996; Ma et al., 1996; Sia et al., 1996). Furthermore, Swe1p accumulation is also periodic during the cell cycle (Fig. 7). In contrast, Mih1p abundance is constant through the cell cycle (McMillan, J.N., and D.J. Lew, unpublished). In the unperturbed cell cycle, G2 cyclin/Cdc28p complexes (the Swe1p substrates) do not accumulate until G2, when Swe1p levels are decreasing, and Swe1p therefore has little effect on the cell cycle. The situation is very different in fission yeast, where *wee1* (homologous to *SWE1*) transcription is constitutive (Aligue et al., 1997) and *cdc25* (homologous to *MIH1*) transcription is periodic, peaking at G2/M (Moreno et al., 1990). With that pattern of regulation, wee1 phosphorylates and inhibits G2 cyclin/cdc2 complexes as soon as they accumulate, and cell cycle progression is delayed until cdc25 accumulates sufficiently to reverse wee1 action. Thus, different programs of regulated transcription contribute to the very different biological roles of the same cell cycle regulators in these two organisms.

The DNA damage checkpoint can delay the cell cycle at multiple stages, depending on when the damage is incurred. This helps to prevent attempts to replicate or segregate damaged DNA, with potentially catastrophic consequences. In contrast, the morphogenesis checkpoint appears to delay the cell cycle specifically in G2, which presumably serves to prevent nuclear division in cells lacking a large enough bud. Once a medium-sized bud has formed, there would no longer be any detriment to going ahead with nuclear division, and wild-type cells no longer delay the cell cycle in response to actin perturbation. We have shown that cells in which *SWE1* transcription has been rendered constitutive (rather than being limited to late G1 and early S phase) delay the cell cycle in response to actin perturbation even in larger-budded cells. Thus, periodic transcription of *SWE1* limits the window within the cell cycle during which actin perturbation can halt cell cycle progression. The consequence of this limitation is that the checkpoint delay is only invoked by the cells that still need more time to complete bud formation.

We thank A. Adams, A. Bretscher, J. Cooper, B. Haarer, and G. Johnston for generously providing strains and plasmids; D. Drubin for a gift of Lat-A; and E. Bi, A. DeLozanne, J. Pringle, B. Nicklas, K. Bloom, and S. Kornbluth for stimulating interactions. Thanks also to E. Bardes for help in preparing the figures.

J.N. McMillan was supported by National Research Service Award GM18455. This work was supported by U.S. Public Health Service grant GM53050 and by funds from the Searle Scholars Program/The Chicago Community Trust to D.J. Lew.

Received for publication 8 January 1998 and in revised form 11 August 1998.

References

Adams, A.E.M., D.I. Johnson, R.M. Longnecker, B.F. Sloat, and J.R. Pringle. 1990. *CDC42* and *CDC43*, two additional genes involved in budding and the establishment of cell polarity in the yeast *Saccharomyces cerevisiae*. *J. Cell Biol.* 111:131–142.

Adams, A.E.M., D. Botstein, and D.G. Drubin. 1991. Requirement of yeast fimbrin for actin organization and morphogenesis *in vivo*. *Nature.* 354:404–408.

Aligue, R., L. Wu, and P. Russell. 1997. Regulation of *Schizosaccharomyces pombe* wee1 tyrosine kinase. *J. Biol. Chem.* 272:13320–13325.

Amatruda, J.F., J.F. Cannon, K. Tatchell, C. Hug, and J.A. Cooper. 1990. Disruption of the actin cytoskeleton in yeast capping protein mutants. *Nature.* 344:352–354.

Amatruda, J.F., D.J. Gattermeir, T.S. Karpova, and J.A. Cooper. 1992. Effects of null mutations and overexpression of capping protein on morphogenesis, actin distribution, and polarized secretion in yeast. *J. Cell Biol.* 119:1151–1162.

Ayscough, K.R., J. Stryker, N. Pokala, M. Sanders, P. Crews, and D.G. Drubin. 1997. High rates of actin filament turnover in budding yeast and roles for actin in establishment and maintenance of cell polarity revealed using the actin inhibitor latrunculin-A. *J. Cell Biol.* 137:399–416.

Booher, R.N., R.J. Deshaies, and M.W. Kirschner. 1993. Properties of *Saccharomyces cerevisiae* wee1 and its differential regulation of p34CDC28 in response to G1 and G2 cyclins. *EMBO (Eur. Mol. Biol. Organ.) J.* 12:3417–3426.

Cannon, J.F., and K. Tatchell. 1987. Characterization of *Saccharomyces cerevisiae* genes encoding subunits of cyclic AMP-dependent protein kinase. *Mol. Cell. Biol.* 7:2653–2663.

Chowdhury, S., K.W. Smith, and M.C. Gustin. 1992. Osmotic stress and the yeast cytoskeleton: phenotype-specific suppression of an actin mutation. *J. Cell Biol.* 118:561–571.

Dean, N., and J.B. Poster. 1996. Molecular and phenotypic analysis of the *S. cerevisiae MNN10* gene identifies a family of related glycosyltransferases. *Glycobiology.* 6:73–81.

DeMarini, D.J., A.E.M. Adams, H. Fares, C. De Virgilio, G. Valle, J.S. Chuang, and J.R. Pringle. 1997. A septin-based hierarchy of proteins required for localized deposition of chitin in the *Saccharomyces cerevisiae* cell wall. *J. Cell Biol.* 139:75–93.

Haarer, B.K., S.H. Lillie, A.E.M. Adams, V. Magdolen, W. Bandlow, and S.S. Brown. 1990. Purification of profilin from *Saccharomyces cerevisiae* and

analysis of profilin-deficient cells. *J. Cell Biol.* 110:105–114.
Haarer, B.K., A.S. Petzold, and S.S. Brown. 1993. Mutational analysis of yeast profilin. *Mol. Cell. Biol.* 13:7864–7873.
Hartwell, L.H., J. Culotti, J.R. Pringle, and B.J. Reid. 1974. Genetic control of the cell division cycle in yeast. *Science.* 183:46–51.
Hartwell, L.H., and T.A. Weinert. 1989. Checkpoints: controls that ensure the order of cell cycle events. *Science.* 246:629–634.
Johnston, G.C., J.A. Prendergast, and R.A. Singer. 1991. The *Saccharomyces cerevisiae MYO2* gene encodes an essential myosin for vectorial transport of vesicles. *J. Cell Biol.* 113:539–551.
Karpova, T.S., M.M. Lepetit, and J.A. Cooper. 1993. Mutations that enhance the *cap2* null mutant phenotype in *Saccharomyces cerevisiae* affect the actin cytoskeleton, morphogenesis and pattern of growth. *Genetics.* 135:693–709.
Lew, D.J., and S.I. Reed. 1993. Morphogenesis in the yeast cell cycle: regulation by Cdc28 and cyclins. *J. Cell Biol.* 120:1305–1320.
Lew, D.J., and S.I. Reed. 1995*a*. A cell cycle checkpoint monitors cell morphogenesis in budding yeast. *J. Cell Biol.* 129:739–749.
Lew, D.J., and S.I. Reed. 1995*b*. Cell cycle control of morphogenesis in budding yeast. *Curr. Opin. Genet. Dev.* 5:17–23.
Lew, D.J., T. Weinert, and J.R. Pringle. 1997. Cell cycle control in *Saccharomyces cerevisiae*. *In* The Molecular and Cellular Biology of the Yeast *Saccharomyces*. J.R. Pringle, J. Broach, and E. Jones, editors. Cold Spring Harbor Laboratory Press, Cold Spring Harbor, NY. 607–695.
Li, J.J., and R.J. Deshaies. 1993. Exercising self-restraint: discouraging illicit acts of S and M in eukaryotes. *Cell.* 74:223–226.
Lillie, S.H., and S.S. Brown. 1994. Immunofluorescence localization of the unconventional myosin, Myo2p, and the putative kinesin-related protein, Smy1p, to the same regions of polarized growth in *Saccharomyces cerevisiae*. *J. Cell Biol.* 125:825–842.
Lim, H.H., P.-Y. Goh, and U. Surana. 1996. Spindle pole body separation in *Saccharomyces cerevisiae* requires dephosphorylation of the tyrosine 19 residue of Cdc28. *Mol. Cell. Biol.* 16:6385–6397.
Liu, H., and A. Bretscher. 1989. Disruption of the single tropomyosin gene in yeast results in the disappearance of actin cables from the cytoskeleton. *Cell.* 57:233–242.
Liu, H., and A. Bretscher. 1992. Characterization of TPM1-disrupted yeast cells indicates an involvement of tropomyosin in directed vesicular transport. *J. Cell Biol.* 118:285–299.
Liu, H., J. Krizek, and A. Bretscher. 1992. Construction of a GAL1-regulated yeast cDNA expression library and its application to the identification of genes whose overexpression causes lethality in yeast. *Genetics.* 132:665–673.
Ma, X.-J., Q. Lu, and M. Grunstein. 1996. A search for proteins that interact genetically with histone H3 and H4 amino termini uncovers novel regulators of the Swe1 kinase in *Saccharomyces cerevisiae*. *Genes Dev.* 10:1327–1340.
Mondesert, G., and S.I. Reed. 1996. *BED1*, a gene encoding a galactosyltransferase homologue, is required for polarized growth and efficient bud emergence in *Saccharomyces cerevisiae*. *J. Cell Biol.* 132:137–151.
Mondesert, G., D.J. Clarke, and S.I. Reed. 1997. Identification of genes controlling growth polarity in the budding yeast *Saccharomyces cerevisiae*: a possible role of N-glycosylation and involvement of the exocyst complex. *Genetics.* 147:421–434.
Moreno, S., P. Nurse, and P. Russell. 1990. Regulation of mitosis by cyclic accumulation of $p80^{cdc25}$ mitotic inducer in fission yeast. *Nature.* 344:549–552.
Murray, A.W. 1992. Creative blocks: cell-cycle checkpoints and feedback controls. *Nature.* 359:599–604.
Navas, T.A., Z. Zhou, and S.J. Elledge. 1995. DNA polymerase epsilon links the DNA replication machinery to the S phase checkpoint. *Cell.* 80:29–39.
Nicklas, R.B., S.C. Ward, and G.J. Gorbsky. 1995. Kinetochore chemistry is sensitive to tension and may link mitotic forces to a cell cycle checkpoint. *J. Cell Biol.* 130:929–939.
Novick, P., and D. Botstein. 1985. Phenotypic analysis of temperature-sensitive yeast actin mutants. *Cell.* 40:405–416.
Paulovich, A.G., and L.H. Hartwell. 1995. A checkpoint regulates the rate of progression through S phase in *S. cerevisiae* in response to DNA damage. *Cell*. 82:841–847.
Pringle, J.R., and L.H. Hartwell. 1981. The *Saccharomyces cerevisiae* cell cycle. *In* The Molecular Biology of the Yeast *Saccharomyces*. J.D. Strathern, E.W. Jones, and J.R. Broach, editors. Cold Spring Harbor Laboratory Press, Cold Spring Harbor, NY. 97–142.
Pringle, J.R., A.E.M. Adams, D.G. Drubin, and B.K. Haarer. 1991. Immunofluorescence methods for yeast. *Methods Enzymol.* 194:565–602.
Pringle, J.R., E. Bi, H.A. Harkins, J.E. Zahner, C. De Virgilio, J. Chant, K. Corrado, and H. Fares. 1995. Establishment of cell polarity in yeast. *Cold Spring Harbor Symp. Quant. Biol.* 60:729–744.
Russell, P., S. Moreno, and S.I. Reed. 1989. Conservation of mitotic controls in fission and budding yeast. *Cell.* 57:295–303.
Sandell, L.L., and V.A. Zakian. 1993. Loss of a yeast telomere: arrest, recovery, and chromosome loss. *Cell.* 75:729–739.
Sia, R.A.L., H.A. Herald, and D.J. Lew. 1996. Cdc28 tyrosine phosphorylation and the morphogenesis checkpoint in budding yeast. *Mol. Biol. Cell.* 7:1657–1666.
Siede, W., A.S. Friedberg, and E.C. Friedberg. 1993. *RAD9*-dependent G1 arrest defines a second checkpoint for damaged DNA in the cell cycle of *Saccharomyces cerevisiae*. *Proc. Natl. Acad. Sci. USA.* 90:7985–7989.
Sikorski, R.S., and P. Hieter. 1989. A system of shuttle vectors and yeast host strains designed for efficient manipulation of DNA in *Saccharomyces cerevisiae*. *Genetics.* 122:19–27.
Toczyski, D.P., D.J. Galgoczy, and L.H. Hartwell. 1997. *CDC5* and CKII control adaptation to the yeast DNA damage checkpoint. *Cell.* 90:1097–1106.
Weinert, T.A., and L.H. Hartwell. 1988. The RAD9 gene controls the cell cycle response to DNA damage in *S. cerevisiae*. *Science.* 241:317–322.
Wells, W.A.E. 1996. The spindle-assembly checkpoint: aiming for a perfect mitosis, every time. *Trends Cell Biol.* 6:228–234.
Yang, S.S., E. Yeh, E.D. Salmon, and K. Bloom. 1997. Identification of a mid-anaphase checkpoint in budding yeast. *J. Cell Biol.* 136:345–354.